

## Elastic Scattering of Low Energy Electrons from Ozone Molecules

Tamayo ONO\*, Etsuko SHIMAKI, Yasuhiko KOJIMA, Yoshitaka KIYAMA,  
Tosiyasu TAKAHASI, Kouichi SOEJIMA and Atsunori DANJO

Graduate School of Science and Technology, Niigata University, Niigata 950-2181

(Received November 17, 2003)

Differential cross sections have been measured for vibrationally elastic scattering of electrons from ozone molecules at incident electron energies from 2 eV to 10 eV in the angular range from 20° to 120°. Absolute values of the differential cross sections have been obtained by means of the relative flow method. Integral and momentum transfer cross sections have been derived from the measured data by extrapolating to 0° and 180° scattering angles. Comparison was made between the present measurements and those from other experiments and theoretical calculations.

KEYWORDS: ozone, electron, elastic scattering, differential cross section

DOI: 10.1143/JPSJ.73.892

### 1. Introduction

Although ozone is only a minor constituent of the earth's atmosphere, it plays an important role in controlling the temperature of the upper atmosphere. In addition, the presence of ozone in the stratosphere is particularly essential to all life as it screens out the biologically harmful ultraviolet radiation. In order to understand various chemical and physical interactions of ozone with radiation and other atmospheric species, we must first have a sound understanding of the properties of the ozone molecule itself. Information on the scattering of electrons from ozone molecules is particularly important for the studies of the fundamental processes in the upper atmosphere.

However, to date only few electron spectroscopic studies of ozone molecules have been reported probably because of the difficulty in preparation and handling of high purity ozone molecular beam and because of its corrosive nature. Pioneering work has been carried out by Celotta *et al.*<sup>1)</sup> and Swanson and Celotta.<sup>2)</sup> Absolute differential cross sections (DCS's) for vibrationally elastic scattering were reported by Shyn and Sweeney<sup>3)</sup> in the electron energy range from 3 eV to 20 eV at the scattering angles from 12° to 156°. Allan *et al.*<sup>4)</sup> have presented absolute DCS's for vibrationally elastic and inelastic scattering of electrons from ozone molecules. Hereafter, "elastic" means "vibrationally elastic", where rotational transitions are not resolved at all. In these two measurements absolute cross sections are obtained with the relative flow method which are originally the same method used in the present experiments. Shyn and Sweeney<sup>3)</sup> normalized their relative DCS's to the standard DCS's for He atoms measured by Shyn.<sup>5)</sup> Allan *et al.*<sup>4)</sup> used the calculated DCS's for He atoms of Nesbet *et al.*<sup>6)</sup> as standard DCS's. Electron energy loss studies of the electronic transitions of ozone molecules have been reported by Allan *et al.*<sup>7)</sup> and Sweeney and Shyn.<sup>8)</sup>

Theoretically, several groups have reported the DCS's for elastic scattering and discussed on the shape resonances in the integral elastic cross sections. Okamoto and Itikawa<sup>9)</sup> have calculated differential, integral and momentum transfer cross sections for elastic scattering of electrons from ozone molecules at four electron energies between 5 eV and

20 eV by employing an effective model potential. Bettega *et al.*,<sup>10)</sup> applying the Swinger multichannel method with pseudopotentials, calculated differential, integral and momentum transfer cross sections for elastic scattering of electrons from ozone molecules at electron energies from 6 eV to 30 eV. Sarpal *et al.*<sup>11)</sup> reported the R-matrix calculations of differential and integral cross sections for elastic scattering of electrons from ozone molecules. Gianturco *et al.*,<sup>12)</sup> using a model local potential with polarization, also reported differential cross sections for elastic scattering in electron–ozone collisions. In these four theoretical calculations, cross sections are given by summing the pure elastic scattering and rotationally inelastic scattering. It is pointed that the rotationally summed cross sections are weakly dependent on the initial rotational state and can be compared with experimental data where rotational features are not resolved.<sup>11,13)</sup>

As described above, very few experiments are available in electron scattering from ozone molecules. Even for the elastic scattering only two measurements have been performed so far.<sup>3,4)</sup> For understandings of physics in collision processes between electrons and ozone molecules we have to study not only elastic scattering but also vibrational and electronic excitations. Apart from this, electron collision processes involving ozone molecules are particularly important for various applied fields. For the first step of systematic studies we have measured absolute DCS's for elastic scattering of electrons from ozone molecules at the incident electron energies below 10 eV. Absolute DCS's give a stringent test for theoretical calculations and serve as a standard for other inelastic processes. In the present measurements we focused on low energy electron collisions with ozone molecules by the following reasons. Some differences, both in magnitude and the shape of the angular distribution, are observed between the previous measurements by Shyn and Sweeney,<sup>3)</sup> and Allan *et al.*<sup>4)</sup> especially at low electron energies below 10 eV. Furthermore, agreement between the measurements and theoretical calculations are also poor in this electron energy range. Hence another experiment is needed. Low energy electron collisions with molecules are important because cross sections are generally large and resonant scattering through negative ion states is expected to enhance the cross sections. For the study of resonant scattering we have to measure cross sections in a

\*E-mail: tamayo@flower.gs.niigata-u.ac.jp

narrow energy step.

## 2. Experimentals

Experimental apparatus and methods used in the present work are similar to those described in our earlier experiment.<sup>14)</sup> The electron spectrometer consists of a hemispherical electrostatic monochromator and the same type of electron energy analyzer. Energy selected electrons are accelerated to the desired electron energy and focused onto the molecular beam at right angles. The molecular beam of ozone is effused through a glass multi-capillary array. The electrons scattered from ozone molecules are energy analyzed and detected by an electron multiplier. The electron analyzer can be rotated in the angular range from  $-30^\circ$  to  $120^\circ$  with respect to the incident electron direction. Elements of the electron spectrometer are made of non-magnetic stainless steel and all slits are made of molybdenum. Magnetic field in the vicinity of the electron spectrometer is reduced to less than 5 mG by two fold  $\mu$ -metal shield. The vacuum chamber is evacuated by a turbomolecular pump. The base pressure in the chamber is  $2 \times 10^{-7}$  Torr and the background pressure is  $2 \times 10^{-6}$  Torr with the molecular beam turned on. The angular resolution of the spectrometer is about  $\pm 2^\circ$ . During the measurements the spectrometer and the nozzle are kept at about  $65^\circ\text{C}$  for the stable operation of the spectrometer.

Schematic drawing of the ozonizer and the gas handling system are shown in Figs. 1(a) and 1(b) respectively. Ozone is prepared by passing pure oxygen stored in the  $\text{O}_2$  bulb through a silent electric discharge tube and the product is immediately liquefied in the bottom of the discharge tube with a liquid  $\text{N}_2$  trap. After the discharge excess oxygen has been pumped away keeping with the liquid  $\text{N}_2$  trap. In this procedure oxygen can be exclusively pumped away because the vapor pressure of oxygen is higher than that of ozone by about 5 orders of magnitude at liquid  $\text{N}_2$  temperature.<sup>15)</sup> After pumping, the liquid  $\text{N}_2$  trap is removed from the discharge tube and another liquid  $\text{N}_2$  trap is supplied to the storage bulb, which is evacuated in advance. Thus, ozone is transferred into the storage bulb. This storage bulb is attached to a gas handling system as shown in Fig. 1(b). Ozone is introduced from the storage glass bulb into the collision region as an effusive beam through the glass multi-capillary array with a thin metal aperture of 1 mm in diameter. The gas handling system is made of glass and poly-tetrafluoroethylene (PTFE) tubings and valves to prevent from the decomposition of ozone molecules.

In order to know the oxygen content in the ozone molecular beam, we have used the same method of Allan *et al.*<sup>4)</sup> to measure the oxygen/ozone ratio. The energy loss spectrum of high purity ozone has been measured at the scattering angle of  $90^\circ$  and at the incident electron energy of 9 eV, where the differential cross section for the vibrational transition from  $v = 0$  to  $v = 1$  of oxygen molecules is large because of the  $\sigma^*$  resonance.<sup>16)</sup> As shown in Fig. 2, the feature of the  $v = 1$  vibrational excitation of oxygen molecules at the energy loss of 0.193 eV has not been observed. When we assume that the signals at 0.193 eV in the energy loss spectrum are due to the  $v = 1$  vibrational excitation of oxygen molecules, the relative number density of oxygen in the sample gas can be written as;

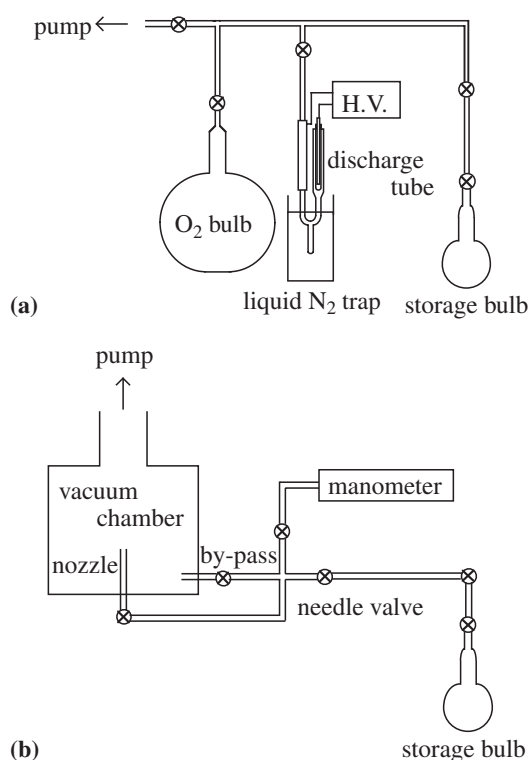


Fig. 1. Schematic drawings of (a) the ozonizer and (b) the gas handling system. The ozonizer and the gas handling system are made of glass and poly-tetrafluoroethylene (PTFE) except for the manometer to prevent from the decomposition of ozone molecules. (a) Ozone is produced by a silent electric discharge at 8 kV (AC) and product ozone is immediately liquefied in the bottom of the discharge tube with a liquid  $\text{N}_2$  trap. After pumping out the excess oxygen, the liquid  $\text{N}_2$  trap is removed from the discharge tube and another liquid  $\text{N}_2$  trap is supplied to the storage bulb, and ozone is transferred into the storage bulb. (b) Ozone is taken from the storage bulb and its flow is regulated with a needle valve, and effused through a nozzle.

$$\frac{N(\text{O}_2)}{N(\text{O}_3)} = \frac{\delta}{1 - \delta} = \frac{h(\text{O}_2)}{h(\text{O}_3)} \times \frac{\text{DCS}(\text{O}_3, \text{elast})(1 - \delta) + \text{DCS}(\text{O}_2, \text{elast})\delta}{\text{DCS}(\text{O}_2, v = 1)} \quad (1)$$

where,  $N(\text{O}_2)$  and  $N(\text{O}_3)$  are the number densities of oxygen and ozone,  $\delta$  is the fraction of oxygen in the sample gas,  $h(\text{O}_2, v = 1)$  and  $h(\text{O}_3, \text{elast})$  are the heights of the oxygen  $v = 1$  signal and the elastic peak, and  $\text{DCS}(\text{O}_2, v = 1)$ ,  $\text{DCS}(\text{O}_3, \text{elast})$  and  $\text{DCS}(\text{O}_2, \text{elast})$  are the oxygen  $v = 1$ , ozone and oxygen elastic DCS's. From the energy loss spectrum in Fig. 2,  $h(\text{O}_2, v = 1)/h(\text{O}_3, \text{elast}) = 108/55,026$  and the values of the DCS's at 9 eV and  $90^\circ$ , which are  $\text{DCS}(\text{O}_2, v = 1) = 0.034 \times 10^{-16} \text{ cm}^2 \text{ sr}^{-1}$ ,<sup>16)</sup>  $\text{DCS}(\text{O}_3, \text{elast}) = 0.5 \times 10^{-16} \text{ cm}^2 \text{ sr}^{-1}$ ,<sup>4)</sup> and  $\text{DCS}(\text{O}_2, \text{elast}) = 0.45 \times 10^{-16} \text{ cm}^2 \text{ sr}^{-1}$ ,<sup>16)</sup>  $\delta = 0.03$ . Hence, the content of oxygen in the molecular beam is estimated to be less than 3%.

The relative flow method developed by Srivastava *et al.*<sup>17)</sup> has been employed to obtain the absolute DCS's. The intensity of the electrons elastically scattered from ozone molecules is measured and immediately followed by the measurements of the electron intensity scattered from He atoms under the same experimental conditions. When the molecular flow through the capillary array is under the condition;

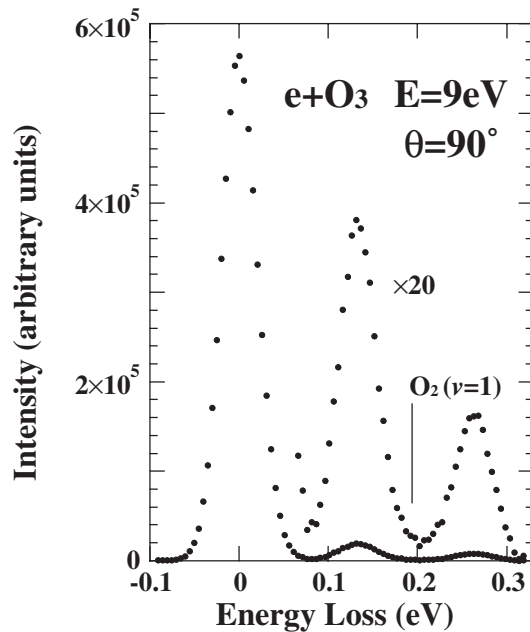


Fig. 2. Energy loss spectrum illustrating the method of determining the oxygen/ozone ratio in the molecular beam. Small two peaks are the features for ozone vibrational excitations and vertical line indicates the position of oxygen  $v = 1$  vibrational excitation ( $\Delta E = 0.193$  eV). From the ratio of the peak heights  $h(\Delta E = 0.193 \text{ eV})/h(\Delta E = 0 \text{ eV})$  and DCS's for elastic scattering from oxygen and ozone molecules, and vibrational excitation of oxygen  $v = 1$ , upper limit of the oxygen content in the molecular beam is estimated to be about 3% (see text).

$$\gamma < K_L < 10, \quad (2)$$

the ratio of the cross sections for elastic scattering from ozone molecules and He atoms is related to the ratio of the two intensities when the electron current is kept constant for both gases;

$$\begin{aligned} \sigma(\text{O}_3; E, \theta) / \sigma(\text{He}; E, \theta) \\ = [N(\text{O}_3; E, \theta) / N(\text{He}; E, \theta)] [p(\text{He}) / p(\text{O}_3)], \end{aligned} \quad (3)$$

where,  $\gamma = D/L$ ,  $K_L = \lambda/L$ ,  $D$  is the diameter and  $L$  the length of the capillary, and  $\lambda$  is the mean free path of ozone molecules and He atoms in the reservoir behind the capillary.<sup>18)</sup>  $\sigma(\text{O}_3; E, \theta)$  and  $\sigma(\text{He}; E, \theta)$  are the DCS's for elastic scattering from ozone molecules and He atoms, and  $N(\text{O}_3; E, \theta)$  and  $N(\text{He}; E, \theta)$  are the rates of the elastically scattered electron intensities at an angle  $\theta$  and an electron energy  $E$ .  $p(\text{O}_3)$  and  $p(\text{He})$  are the pressures of ozone molecules and He atoms in the reservoir. However, under the molecular flow condition it is difficult to conduct the electron scattering experiments due to low target gas density. Hence, Trajmar and Register<sup>18)</sup> have recommended the operating conditions for various gases with the capillary array with  $\gamma = 0.01$  when the relative flow calibrations are made against He atoms. Following their recommendation we used  $p(\text{O}_3) = 1$  Torr and  $p(\text{He}) = 4$  Torr for equal Knudsen numbers  $K_L$ , and these pressures were measured by a capacitance manometer in the present measurements. The diameter and length of the capillary in the present experiments are  $D = 12 \mu\text{m}$  and  $L = 1$  mm, and hence the above inequality (2) is fulfilled in our case with  $\lambda = 35 \mu\text{m}$ . The electron optics was carefully adjusted to avoid changes in surface potentials when working with different gases. The

intensity of the primary electron beam is monitored with a Faraday cup and typical electron current is 1 nA. The electron beam direction is carefully tuned so that the scattered electron intensity gives a symmetrical distribution with respect to the  $0^\circ$  scattering angle.

The incident electron energy scale was calibrated with an accuracy of  $\pm 20$  meV by observing the well-known  $^2\Pi_g$   $\text{N}_2^-$  shape resonance around 2–3 eV in elastic cross sections. The determination of the peak positions was referred to Rohr.<sup>19)</sup> Energy resolution of the present spectrometer is about 40 meV in full width at half maximum (FWHM).

Scattered electron intensities from ozone molecules and He atoms are obtained by subtracting the background electron intensities measured at the corresponding scattering angle. In the background measurements ozone molecules are introduced through the by-pass shown in Fig. 1(b) so as to give the same base pressure in the chamber as in the case from the nozzle. Statistical uncertainties are less than 3% and background electrons are negligibly small except at  $20^\circ$  scattering angle. The error from the relative readings of the pressure of ozone molecules or He atoms and its fluctuation is estimated to be 5%. Another 5% error comes from the incident electron current measurements. It is difficult to estimate the error due to the change of the collision volume through the gas replacement, because the spatial distribution of the electron beam is not monitored in the present measurements. We assume 10% error with the collision volume. The error of the standard He DCS's by Boesten and Tanaka<sup>20)</sup> is claimed to be 10%. The resultant error of the present elastic DCS's, taken as the quadrature sum of the components, is about 16% except for the lowest scattering angle of  $20^\circ$ , where background subtraction makes the statistics worse. It causes a further uncertainty into the  $20^\circ$  DCS's to give an overall error of about 20% at the lowest angles.

### 3. Results and Discussions

Figure 3 shows a typical energy loss spectrum at the electron energy of 4 eV and scattering angle of  $30^\circ$ . Ozone has three fundamental modes of vibration, i.e. a bending mode  $v_2$ , a symmetric stretching mode  $v_1$  and an antisymmetric mode  $v_3$ . Vertical bars in the figure show the progressions of three modes which are taken from the review article of Steinfeld *et al.*<sup>21)</sup> Transitions from rotationally excited states of ozone molecules also contribute to the elastic feature in the present measurements at  $65^\circ\text{C}$ , and this effect is about 5% larger compared to the measurements at  $20^\circ\text{C}$ . The energy resolution of the spectrometer is about 40 meV in full width at half maximum (FWHM), sufficient to resolve the elastic peak from the vibrational excitations. However any rotational transition is not resolved at all, hence, rotationally summed cross sections are presented.

Absolute DCS's for elastic scattering of electrons from ozone molecules have been measured at incident electron energies from 2 eV to 10 eV in the angular range from  $20^\circ$  to  $120^\circ$ . Absolute values of the DCS's are tabulated in Table I. For comparison with previous experimental or calculated integral cross sections and momentum transfer cross sections, the measured DCS's in the limited angular range have to be extrapolated both to smaller and larger angles. We have no established method for extrapolation at present.

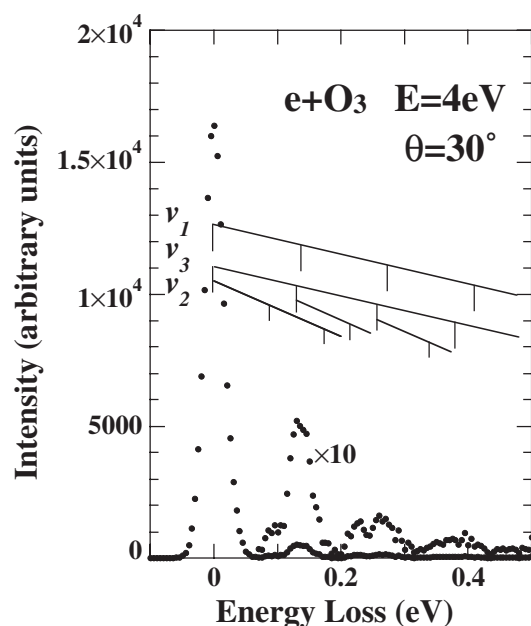


Fig. 3. Energy loss spectrum of electrons scattered from ozone molecules at the electron energy of 4 eV and scattering angle of 30°. Vertical lines show the progressions of three vibrational modes, a bending mode  $v_2$ , a symmetric stretching mode  $v_1$  and an antisymmetric mode  $v_3$  which are taken from the review article of Steinfeld *et al.*<sup>21)</sup>

Although the present extrapolations are rather arbitrary, integral and momentum transfer cross sections are derived by extrapolating the measured data to smaller and larger angles, which are also given at the bottom of the table.

For an example, the extrapolated cross sections are shown by small solid circles in Fig. 6, and two extreme cases, upper and lower extrapolations, are also shown by small open circles. The insert shows the extrapolation to small angles. At 10 eV, the upper extrapolation gives larger values by 8% for the integral cross section ( $Q_I$ ) and 12% for the momentum transfer cross section ( $Q_M$ ) than the values listed in Table I. On the other hand the lower extrapolation gives smaller values for  $Q_I$  by 6% and for  $Q_M$  by 10%. Hence,

Table I. Elastic DCS's in  $10^{-16} \text{ cm}^2 \text{ sr}^{-1}$ , and integral cross sections  $Q_I$  and momentum transfer cross sections  $Q_M$  in  $10^{-16} \text{ cm}^2$ .

Angle (deg)	Electron energy (eV)							
	2	3	4	5	6	7	8	10
20	1.3	1.3	1.5	2.2	2.1	2.5	2.4	3.0
30	0.79	0.91	1.2	1.8	1.9	2.0	2.2	2.2
40	0.76	0.90	1.3	1.6	1.9	1.8	1.9	1.8
50	0.68	0.89	1.2	1.7	1.5	1.5	1.7	1.6
60	0.87	1.0	1.1	1.4	1.3	1.3	1.3	1.1
70	0.86	0.99	1.1	1.2	1.1	1.0	1.1	0.83
80	0.85	0.84	0.88	1.0	0.78	0.74	0.77	0.64
90	0.86	0.77	0.80	0.79	0.68	0.64	0.62	0.58
100	0.73	0.73	0.67	0.60	0.53	0.54	0.57	0.51
110	0.60	0.73	0.67	0.56	0.47	0.51	0.58	0.52
120	0.53	0.65	0.74	0.57	0.58	0.54	0.56	0.60
$Q_I$	9.1	10	12	13	13	13	13	14
$Q_M$	7.6	9.3	11	9.7	9.9	9.4	9.3	10

errors due to the extrapolations are estimated to be 8% for  $Q_I$  and 12% for  $Q_M$ . Quadrature sum of these errors and 20% errors for the DCS's gives 22% and 24% errors for the integral and momentum transfer cross sections respectively.

Figure 4 shows the DCS's for elastic scattering of electrons at (a) 2 eV and (b) 3 eV incident electron energies along with the available experimental and theoretical results. Typical error bar is given at 90°. A broad cross section maximum can be seen at around 80° in the present DCS's at 2 eV incident electron energy and it shifts to around 60° at 3 eV. The present DCS's at 2 eV incident electron energy show good agreement with the measurements by Allan *et al.*<sup>4)</sup> except for small differences at small and large scattering angles, where the present DCS's give slightly steeper angular dependence than their results. It is noted that the standard He DCS's by Boesten and Tanaka,<sup>20)</sup> which are used for the present normalization, are in excellent agreement with those used by Allan *et al.*<sup>4)</sup> Situations are the same for other electron energies. Theoretical calculations by Sarpal *et al.*<sup>11)</sup> well reproduce the experimental results in the

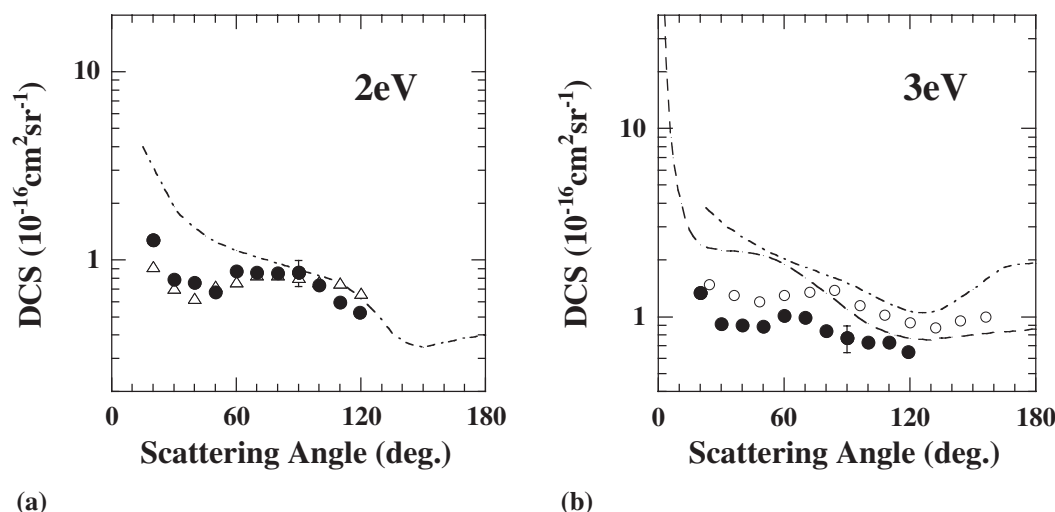


Fig. 4. Absolute differential cross sections for elastic scattering from ozone molecules at electron energies of (a) 2 eV and (b) 3 eV. Solid circles, present experimental results; open circles, experimental results of Shyn and Sweeney;<sup>3)</sup> open triangles, experimental results of Allan *et al.*<sup>4)</sup> dot-dashed curve, calculated results of Sarpal *et al.*<sup>11)</sup> dashed curve, calculated results of Gianturco *et al.*<sup>12)</sup>



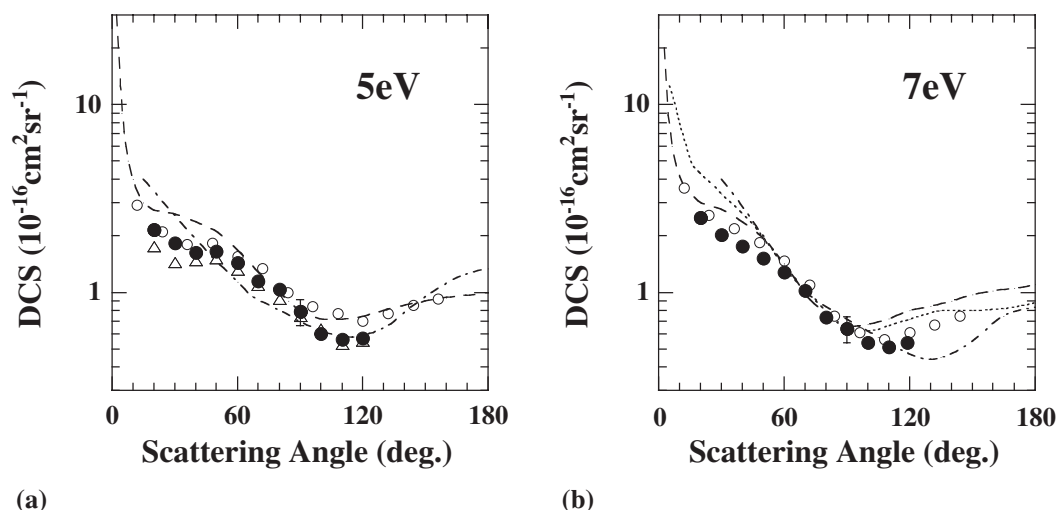


Fig. 5. Absolute differential cross sections for elastic scattering from ozone molecules at electron energies of (a) 5 eV and (b) 7 eV. Solid circles, present experimental results; open circles, experimental results of Shyn and Sweeney;<sup>3)</sup> open triangles, experimental results of Allan *et al.*;<sup>4)</sup> broken curve, calculated results of Bettega *et al.*;<sup>10)</sup> dot-dashed curve, calculated results of Sarpal *et al.*;<sup>11)</sup> dashed curve, calculated results of Gianturco *et al.*<sup>12)</sup>

scattering angles between 70° to 120°. However, their results are much higher than the present measurements at small scattering angles. Sarpal *et al.*<sup>11)</sup> postulate that a correct treatment of electron correlations, including electronic excitation, will be necessary to improve agreement in this angular region. At 3 eV incident electron energy, the present DCS's are systematically smaller than the results of Shyn and Sweeney<sup>3)</sup> by about 30%, though both of the standard He DCS's are in good agreement. The theoretical calculations by Gianturco *et al.*<sup>12)</sup> reproduce the experimental angular dependence fairly well, though their DCS's are higher than the experimental results at small scattering angles.

Figure 5 shows the DCS's at (a) 5 eV and (b) 7 eV incident electron energies along with the experimental and theoretical results. The cross section maximum observed at 2 and 3 eV becomes less enhanced at 5 eV. The present DCS's at 5 eV incident electron energy are again in good agreement with those of Allan *et al.*<sup>4)</sup> but their result are slightly lower than the present measurements at small scattering angles. The measurements by Shyn and Sweeney<sup>3)</sup> are also in good agreement with the present results, giving slightly higher cross sections at large scattering angles. Agreement between the present DCS's and the calculations by Sarpal *et al.*<sup>11)</sup> and Gianturco *et al.*<sup>12)</sup> is fairly well throughout the whole scattering angles. The present DCS's at 7 eV incident electron energy are in excellent agreement with the experimental results of Shyn and Sweeney<sup>3)</sup> over the whole scattering angles. The calculated DCS's by Gianturco *et al.*<sup>12)</sup> agree well with the experimental results, though their results are slightly higher than the measurements.

Figure 6 shows the DCS's at 10 eV incident electron energy together with the measurements by Shyn and Sweeney<sup>3)</sup> and Allan *et al.*<sup>4)</sup> and the theoretical predictions by Bettega *et al.*,<sup>10)</sup> Sarpal *et al.*<sup>11)</sup> and Gianturco *et al.*<sup>12)</sup> As described above, the extrapolated cross sections with two extreme cases are shown in the figure. All the measurements are in good agreement with each other over the measured angular range, and agreement between the measurements and the theoretical predictions by Bettega *et al.*<sup>10)</sup> and Sarpal

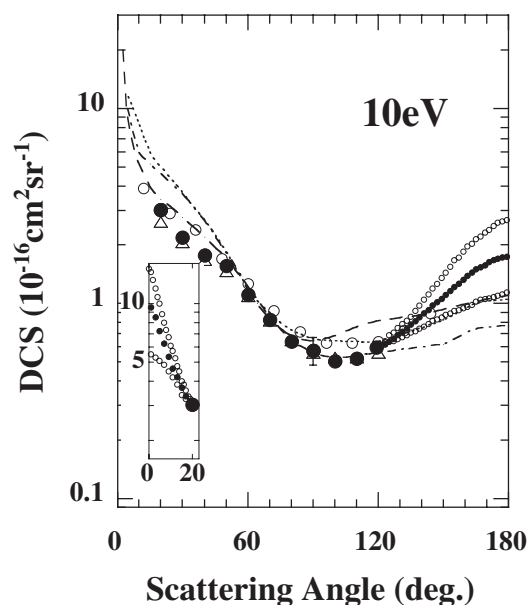


Fig. 6. Absolute differential cross sections for elastic scattering from ozone molecules at electron energy of 10 eV. For an example, the extrapolated cross sections are shown by small solid circles, and two extreme cases, upper and lower extrapolations, are also shown by small open circles. The insert shows the extrapolation to small angles. Solid circles, present experimental results; open circles, experimental results of Shyn and Sweeney;<sup>3)</sup> open triangles, experimental results of Allan *et al.*;<sup>4)</sup> broken curve, calculated results of Bettega *et al.*;<sup>10)</sup> dot-dashed curve, calculated results of Sarpal *et al.*;<sup>11)</sup> dashed curve, calculated results of Gianturco *et al.*<sup>12)</sup>

*et al.*<sup>11)</sup> are very well except at small scattering angles, where theories give still higher cross sections. The theoretical calculations by Gianturco *et al.*<sup>12)</sup> reproduce the measurements very well at the scattering angles below 90° with slightly high cross sections at large scattering angles.

Figure 7(a) shows the integral cross sections along with the experimental results of Shyn and Sweeney<sup>3)</sup> and the theoretical calculations. Typical error bar is given at 3 eV. The integral cross sections are almost constant from 5 eV to 10 eV, and below 5 eV they decrease with decrease of the

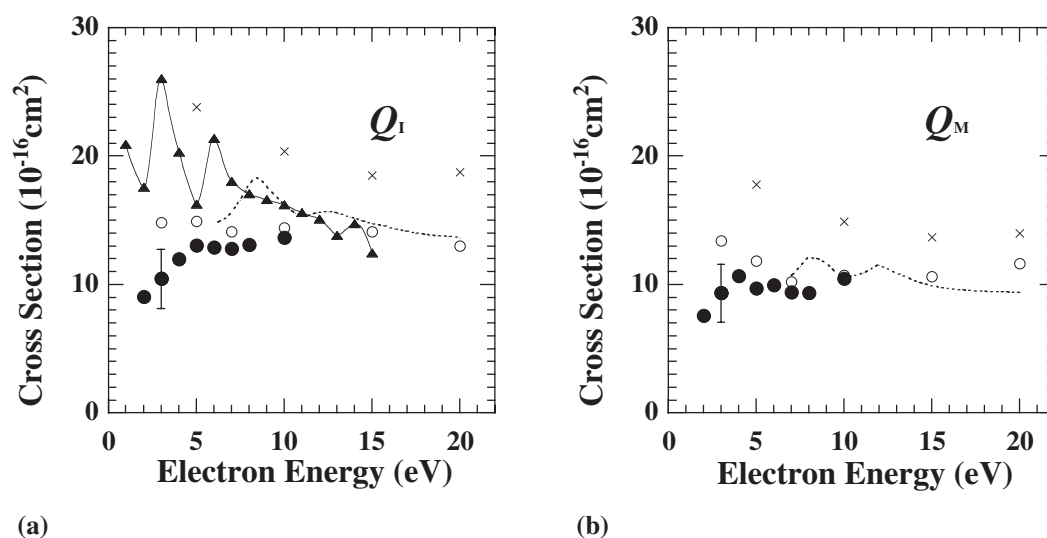


Fig. 7. (a) Integral cross sections for elastic scattering and (b) momentum transfer cross sections. Solid circles, present experimental results; open circles, experimental results of Shyn and Sweeney;<sup>3)</sup> crosses, calculated results of Okamoto and Itikawa;<sup>9)</sup> broken curve, calculated results of Bettega *et al.*;<sup>10)</sup> solid triangles with line, calculated results of Sarpal *et al.*<sup>11)</sup> (line is only for the guide of eyes).

electron energy. Energy dependence of the present cross sections is rather smooth though errors are rather large, indicating less contribution of the resonances. The present results are in good agreement with those of Shyn and Sweeney<sup>3)</sup> except at their lowest energy of 3 eV, being higher than the present results. Theoretical calculations of Sarpal *et al.*<sup>11)</sup> give higher values than the present measurements especially at low electron energies. These values are taken from Table 3 in their paper.<sup>11)</sup> In the theoretical predictions, the enhancement of the cross sections due to shape resonances are observed. However they are located at different energies, and hence further theoretical works are needed.

Figure 7(b) shows momentum transfer cross sections along with the experimental results of Shyn and Sweeney<sup>3)</sup> and the theoretical predictions by Okamoto and Itikawa<sup>9)</sup> and Bettega *et al.*<sup>10)</sup> The present results are again in good agreement with those of Shyn and Sweeney<sup>3)</sup> except at their lowest electron energy. The theoretical predictions by Okamoto and Itikawa<sup>9)</sup> are higher than the measurements. The theoretical results by Bettega *et al.*<sup>10)</sup> agree well with the measurements.

#### 4. Conclusion

We have presented the absolute differential cross sections for elastic scattering of electrons from ozone molecules at scattering angles from 20° to 120° and electron energies from 2 to 10 eV basically in 1 eV step. The present DCS's are in good agreement with the previous measurements except at 3 eV. Some discrepancies are seen at small scattering angles between the measurements and the theoretical calculations as discussed in §3. In the present cross sections for elastic scattering from ozone molecules, structures due to resonances are not observed, which are predicted by theories. For further discussions, both exper-

imental and theoretical studies are needed.

#### Acknowledgements

This work was supported by a Grant-in-Aid for Scientific Research from the Ministry of Education, Culture, Sports, Science and Technology of Japan.

- 1) R. J. Celotta, S. R. Mielczarek and C. E. Kuyatt: *Chem. Phys. Lett.* **24** (1974) 428.
- 2) N. Swanson and R. J. Celotta: *Phys. Rev. Lett.* **35** (1975) 783.
- 3) T. W. Shyn and C. J. Sweeney: *Phys. Rev. A* **47** (1993) 2919.
- 4) M. Allan, K. R. Asmis, D. B. Popovic, M. Stepanovic, N. J. Mason and J. A. Davies: *J. Phys. B* **29** (1996) 4727.
- 5) T. W. Shyn: *Phys. Rev. A* **22** (1980) 916.
- 6) R. K. Nesbet: *Phys. Rev. A* **20** (1979) 58.
- 7) M. Allan, N. J. Mason and J. A. Davies: *J. Chem. Phys.* **105** (1996) 5665.
- 8) C. J. Sweeney and T. W. Shyn: *Phys. Rev. A* **53** (1996) 1576.
- 9) Y. Okamoto and Y. Itikawa: *Chem. Phys. Lett.* **203** (1993) 61.
- 10) M. H. F. Bettega, M. T. do N. Varella, L. G. Ferreira and M. A. P. Lima: *J. Phys. B* **31** (1998) 4419.
- 11) B. K. Sarpal, B. M. Nestmann and S. D. Peyerimhoff: *J. Phys. B* **31** (1998) 1333.
- 12) F. A. Gianturco, P. Paoletti and N. Sanna: *Phys. Rev. A* **58** (1998) 4484.
- 13) Y. Okamoto, K. Onda and Y. Itikawa: *J. Phys. B* **26** (1993) 745.
- 14) H. Nishimura, A. Danjo and H. Sugahara: *J. Phys. Soc. Jpn.* **54** (1985) 1757.
- 15) S. Hosokawa and S. Ichimura: *Rev. Sci. Instrum.* **62** (1991) 1614.
- 16) M. Allan: *J. Phys. B* **28** (1995) 5163.
- 17) S. K. Srivastava, A. Chutjian and S. Trajmar: *J. Chem. Phys.* **63** (1975) 2659.
- 18) S. Trajmar and D. F. Register: *Electron-Molecule Collisions*, ed. I. Shimamura and K. Takayanagi (Plenum Press, New York, 1984) Chap. 6, pp. 468–469.
- 19) K. Rohr: *J. Phys. B* **10** (1977) 2215.
- 20) L. Boesten and H. Tanaka: *At. Data Nucl. Data Tables* **52** (1992) 25.
- 21) J. I. Steinfeld, S. M. Adler-Golden and J. W. Gallagher: *J. Phys. Chem. Ref. Data* **16** (1987) 911.